



Study of silver nanoparticles bioaccumulation in cultured red and green seaweed

Juan José López-Mayán^a, Blanca Álvarez-Fernández^a, Elena Peña-Vázquez^a,
María Carmen Barciela-Alonso^{a,*}, Antonio Moreda-Piñeiro^a, Julie Maguire^b, Mick Mackey^b,
Pilar Bermejo-Barrera^a

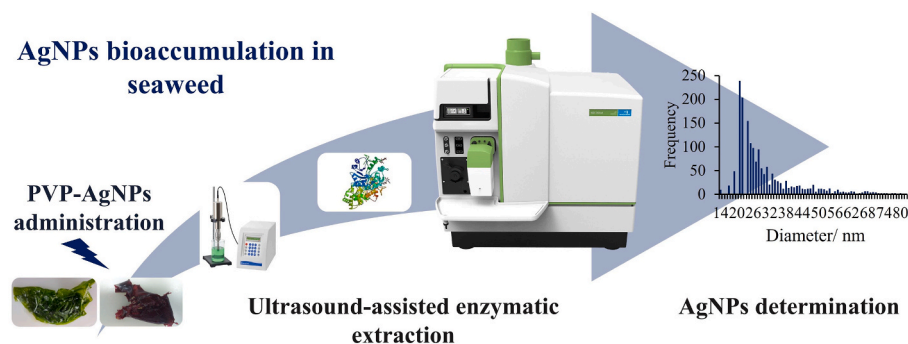
^a Trace Element, Spectroscopy and Speciation Group (GETEE), Instituto de Materiais (iMATUS), Faculty of Chemistry, University of Santiago de Compostela, Av. das Ciencias, s/n 15782, Santiago de Compostela, Spain

^b Indigo Rock Marine Research Station, Gearhies, Bantry, Co. Cork, P75 AX07, Ireland

HIGHLIGHTS

- Green and red seaweed were exposed to 0.1 and 1.0 mg L⁻¹ of 15 nm AgNPs for 28 days.
- Enzymatic extraction and SP-ICP-MS were used for AgNPs determination.
- Both types of seaweed bioaccumulated AgNPs at different rates.
- Total Ag and AgNPs did not increase proportionally to exposure concentration.
- The levels of Ag in exposed seaweed were lower than those found in previous studies.

GRAPHICAL ABSTRACT



ARTICLE INFO

Handling editor: Magali Houde

Keywords:

Seaweed
Palmaria palmata
Ulva sp.
Silver nanoparticles
Bioaccumulation
Single particle Inductively Coupled Plasma
Mass Spectrometry

ABSTRACT

The bioaccumulation of polyvinylpyrrolidone-coated silver nanoparticles (PVP-AgNPs) in *Palmaria palmata* and *Ulva* sp. seaweed was investigated by ICP-MS and SP-ICP-MS (determination of nanoparticles and size distribution after an enzymatic extraction). Seaweeds were exposed to 0.1 and 1.0 mg L⁻¹ of PVP-AgNPs of small particle size (15 nm) for 28 days. They were cultured in 40-L seawater tanks and nanoparticles were mixed with growing media and the phytoplankton used for feeding.

Bioaccumulation changed with the type of seaweed and was not proportional to the concentration. *Palmaria palmata* and *Ulva* sp. reached the maximum total Ag concentration at 14 and 21 days of exposure to 1.0 mg L⁻¹, respectively. The Ag concentrations measured (until 0.79 ± 0.06 µg g⁻¹ w.w.) were much smaller than those found in previous studies after short-term exposure (up to 48 h) under laboratory conditions, probably due to the presence of organic matter in the growing media. The maximum concentrations of AgNPs were achieved at 14 and 28 days for *Palmaria palmata* and *Ulva* sp., respectively, with most frequent sizes of approximately 20 nm. The size values measured by SP-ICP-MS agreed with TEM sizes in the enzymatic extracts. No changes were observed in the concentrations of most metals (Co, Cr, Cu, Mo, Ni, Rb and V) in exposed seaweed; only a decrease of Cd and Pb at the dose of 1 mg L⁻¹ in *Palmaria* was observed.

* Corresponding author.

E-mail address: mcarmen.barciela@usc.es (M.C. Barciela-Alonso).

<https://doi.org/10.1016/j.chemosphere.2024.143872>

Received 30 July 2024; Received in revised form 29 November 2024; Accepted 30 November 2024

Available online 9 December 2024

0045-6535/© 2024 The Authors. Published by Elsevier Ltd. This is an open access article under the CC BY-NC license (<http://creativecommons.org/licenses/by-nc/4.0/>).

Studies simulating the real marine environment are important to estimate bioaccumulation and safety, which change depending on the type of seaweed and nanoparticle.

1. Introduction

In the last decade, nanotechnology has experienced exponential growth and engineered nanomaterials (ENMs) are being massively employed in several sectors due to their novel properties in comparison to bulk materials. Silver nanoparticles (AgNPs) are one of the most widely used ENMs in the industry due to their bactericidal, antifungal and anticancer properties (Wei et al., 2015; Pulit-Prociak et al., 2015; Vimbela et al., 2017; Banerjee and Roychoudhury, 2019), with many application fields including medicine, drug delivery, odontology, health care, textiles, water and air purification, electronics, biosensing, and food production among others (Tortella et al., 2020; Tran et al., 2013; Chernousova and Epple, 2013).

The proliferation of applications and products containing NPs inevitably results in the release of these materials into the environment, (e. g., surface/groundwater, soils/sediments, atmosphere, and marine environments) (Wang et al., 2014) increasing their concentration, and being considered as potential emerging contaminants. In addition, AgNPs can change in size and shape, react with other species, dissolve in contact with water and can even be taken up by living organisms and thus be transferred through the trophic chain, including humans. In marine sediments, different chemical species may be formed (Ag_2S , AgCl , and Ag^0) (Wang et al., 2014; Levard et al., 2012). Several studies proposed that AgNPs toxicity to bacteria is produced through different mechanisms including: 1) the formation of reactive oxygen species (ROS) such as O_2 (Levard et al., 2012; Choi and Hu, 2008), and 2) the interaction of Ag ions with thiol groups of enzymes and proteins affecting cellular respiration, transport of ions through membranes, and causing cellular death (Hwang et al., 2008). Other studies demonstrated the AgNPs toxicity in terrestrial plants (*Lolium multiflorum*) (Yin et al., 2011), aquatic plants (*Lemna minor*) (Gubbins et al., 2011), fungi and algae (Navarro et al., 2008), vertebrates (zebrafish) (Asharani et al., 2008), and even human cells (glioblastoma cells, lung fibroblast cells, and skin keratinocytes) (Valdiglesias, 2022; Lu et al., 2010). Although the toxicity of AgNPs is partly explained by the release of Ag ions, it remains unclear if AgNPs are a direct cause of enhanced toxicity (Levard et al., 2012). Some studies were also carried out to evaluate the AgNPs bioaccumulation and toxicity on different microalgae (*Chlamydomonas reinhardtii*) (Chae and An, 2016; McTeer et al., 2014), (*Raphidocelis subcapitata*) (Lekamge et al., 2020; Ribeiro et al., 2015), (*Mycrocystis auroginosa*) (Xiang et al., 2018), (*Pseudokirchneriella subcapitata*) (Książczyk et al., 2015), (*Chlorella vulgaris*) (Zhang et al., 2020).

Seaweeds can accumulate metals and other pollutants (organic compounds, trace elements, even nanomaterials) (Ali et al., 2021; Bonanno and Orlando-Bonaca, 2018; Sinaei et al., 2018) from seawater, and they can be used as bioindicators of environmental pollution. However, there are scarce data on the fate of metal engineered nanoparticles in estuaries, their toxicity and bioaccumulation pathways under lab and environmental conditions, with most of the previous literature focusing on mollusks and bacteria (Arienzo and Ferrara, 2022). Turner et al., 2012 studied the accumulation and the toxicity of silver nanoparticles (58 ± 27 nm) and dissolved Ag exposing the macroalga *Ulva lactuca* to AgNPs and AgNO_3 for 48 h. In addition, Sfriso et al., 2019 reported the toxicity of citrate-coated AgNPs (35 ± 9 nm) and AgNO_3 in seawater *Ulva rigida* C. Agardh. The toxic effects (chloroplast damage, oxidative stress, lipid peroxidation) were verified by TEM microscopy after 24 h exposure to AgNPs. (Siddiqui and Bielmeyer-Fraser, 2019) compared the accumulation and effects of silver nitrate and silver oxide nanoparticles (40–70 nm) in a green seaweed (*Ulva lactuca*) and a red seaweed (*Agardhiella subulata*) for 24 h.

Moreover, seaweed is an increasingly demanded foodstuff in Europe due to changes in eating styles (towards vegetarian, vegan and sustainable diets), being a natural source of fiber, vitamin B-12, lipids, selenium, fatty acids (including Omega-3), iodine, and antioxidants (polyphenols, carotenoids and tocopherols) (Gómez-Ordóñez et al., 2010; Cofrades et al., 2010). Nanoparticles in the aquatic media could be assimilated by marine organisms, like seaweed, be bioaccumulated or be transformed into other species and be transferred through the food chain, reaching humans. The study of their accumulation in edible algae is important to assess the health risk of their consumption. On the other hand, algae are also used as fertilizers to enlarge crop yields and quality in sustainable agriculture (Pei et al., 2024). The addition of seaweed can increase the amount of organic matter in the soil, regulate the pH, reduce the ratio of C/N in sandy soils, and even regulate heavy metal content (Ammar et al., 2022). However, a high content of Ag or AgNPs in such fertilizers could increase their concentration in the growing soil and consequently in the plants.

Although there are some reports on the bioaccumulation and toxicity of AgNPs in microalgae, to the best of our knowledge, there are no detailed studies about the patterns of AgNPs bioaccumulation in edible macroalgae during long exposure times (>48 h) to nanoparticles sizes lower than 20 nm (nanoparticle bactericidal power is size-dependent with a negative correlation, Liao et al., 2019). Therefore, this research work aims to study the bioaccumulation of PVP-coated AgNPs in two species of edible macroalgae (*Palmaria palmata* and *Ulva* sp.) from the Atlantic area exposed to two different doses for 28 days in seawater containing growing media. The variation in the trend of total Ag and nanoparticulate content (number and AgNPs size distribution) with exposure time was evaluated by inductively coupled plasma mass spectrometry (ICP-MS) and single-particle-ICP-MS (SP-ICP-MS), respectively.

2. Materials and methods

2.1. Instrumentation

• Sample preparation

An Ethos Plus microwave lab station (Milestone, Bergamo, Italy) was used for seaweed sample digestion. The microwave is equipped with ten Teflon vessels (100 mL), Teflon covers, an HTC adapter plate, HTC safety springs (Milestone), and a pressure and temperature controller probe. A Boxcult temperature-controlled incubation chamber (Stuart Scientific, Surrey, UK) equipped with a Rotabit orbital-rocking platform shaker (J. P. Selecta, Barcelona, Spain) was used for AgNPs extraction.

• Total Ag and AgNPs determination

An inductively coupled plasma mass spectrometer (ICP-MS) NexION® 2000 (PerkinElmer, Waltham, MA, USA) with Kinetic Energy Discrimination (KED) was used for total Ag determination. Single-particle mode (SP-ICP-MS) was used with the Syngistix™ Nano Application 2.5 software (PerkinElmer) to obtain AgNPs concentration and size distributions.

• Characterization of AgNPs

A scanning transmission electron microscopy (STEM) with a probe-corrected FEI Titan G2 80–200 kV ChemiSTEM (FEI, Hillsboro, USA) was employed for the characterization of AgNPs in the enzymatic

extracts.

- Other instrumentation

Other instrumentation includes: a VibraCell™ VCX 130 V (Sonics Newtown, CT, USA), a pH meter Basic20 (Crison, Barcelona, Spain), VWR Ultrasonic Cleaner (Barcelona, Spain), a Reax top vortex vibrational shaker (Heidolph, Schwabach, Germany), a 2K15 centrifuge (Sigma, Osterode, Germany), and an analytical balance ML204 (Mettler Toledo, Barcelona, Spain) were used for sample preparation.

2.2. Reagents and materials

- Bioaccumulation assay

To perform the bioaccumulation assay and feed the seaweed, a polyvinylpyrrolidone (PVP) coated Ag nanopowder of 15 nm and a concentration of 5.4×10^{14} particles mL^{-1} from SkySpring Nanomaterials, Inc. (Houston, TX, USA) was used.

- Sample preparation for Ag total determination

Nitric acid 69% (w/v) (SUPRAPUR®, Sigma Aldrich, Darmstadt, Germany) and 33% (v/v) hydrogen peroxide (ACS, ISO, AppliChem Panreac, Barcelona, Spain) were used for microwave sample digestion.

- Nanoparticle extraction

To isolate AgNPs from the seaweed matrix, a Macerozyme® R-10 enzyme mixture (Merck, Darmstadt, Germany) was used. It is formed by pectinase (0.5 units per mg), cellulase (0.1 units per mg), and hemi-cellulase (0.25 units per mg), and it is obtained from *Rhizopus* sp.

Trisodium citrate di-hydrated for analysis (Merck, Darmstadt, Germany) and citric acid for analysis (ACS, Panreac, Barcelona, Spain) were used for buffer preparation.

- Analysis of total Ag and AgNPs

To prepare the ionic Ag standards, an ionic Ag stock solution (1000 mg L^{-1}) in 2% HNO_3 (PerkinElmer, Shelton, CT, USA) was used, whereas an ionic Rh stock solution (1000 mg L^{-1}) in 2% HCl (PerkinElmer, Shelton, CT, USA) was diluted before use as an internal standard. 1% v/v glycerol (Merck, Darmstadt, Germany) was used for extract dilution before analysis by SP-ICP-MS.

An ionic Au stock standard (1000 mg L^{-1}) in 2 mol L^{-1} HCl (Merck), and a reference material PEG-COOH Gold Nanospheres (49.6 nm and 9.89×10^6 particles mL^{-1}) from NanoComposix (San Diego, CA, USA), were used for transport efficiency calculations in SP-ICP-MS.

- Sample preparation for STEM analysis

Regenerated cellulose Amicon Ultra-0.5 mL centrifugal filter units of 30 kDa nominal molecular weight limit (Merck, Darmstadt) were employed to clean the seaweed enzymatic extracts before AgNPs characterization by STEM.

- Other reagents and materials

Other reagents were used to perform the analysis by ICP-MS. They included NexION Setup Solution ($1.0 \mu\text{g L}^{-1}$ of Be, Ce, Fe, In, Li, Mg, Pb, and U in 1% of HNO_3) from PerkinElmer; He and Ar, both with a 99.999% of purity, were from Nippon Gases (Madrid, Spain). Stock standards solutions of 1000 mg L^{-1} of As, Cd, Co, Cr, Cu, Ni, Pb, Rb, Se, V and Zn (PerkinElmer), Mo and Sb (Merck) were diluted to determine the metallic content in the acidic digests of the seaweed at the different dose and exposure times.

Other materials included plasticware (e.g. tubes, pipette tips, and syringes) and Minisart NML hydrophilic non-sterile 5.0 μm filters (Sartorius, Goettingen, Germany). Ultrapure water (18 M Ω cm of resistivity) was obtained from a Milli-Q® IQ7003 (Millipore Co., Bedford, MA, USA) purification system.

2.3. Seaweed culture and exposure to AgNPs

Palmaria palmata (red seaweed) and *Ulva* sp. (green seaweed) were cultured at Indigo Rock Marine Research Centre (Cork, Ireland). Both seaweed species were exposed to 15 nm PVP-AgNPs at two different nominal doses (0.1 and 1.0 mg L^{-1}) for 28 days.

Seaweeds were cultured in 40 L tanks at $15 \pm 1 \text{ }^\circ\text{C}$ with periods of 12 h of white light and 12 h of darkness. Parameters like pH, temperature, dissolved O_2 , and salinity were measured every day. However, conductivity, ammonium, and nitrites were tested twice a week. The seaweeds were fed using cell-Hi F2P growth medium (a soluble nutrient blend commonly used in the production of marine microalgae). Each tank received 30 mL of the F2P medium (0.1 g mL^{-1}) three times a week following the total and partial water changes. A total water change was conducted on the day of the trial, after all algal samples were extracted and processed, and before the addition of the nanoparticles. Fifty per cent of the water was replaced twice per week, two days before and two days after the addition of nanoparticles. The nanoparticles were resuspended using an ultrasonic bath and added once per week with the F2P medium by micro pipetting and manual shaking to obtain the final concentration in the low and high dose tanks (i.e. 0.1 and 1.0 mg L^{-1} , respectively). Three control tanks (A-C: seaweed in growing medium without nanoparticles), three solvent control tanks (D-F: seaweed exposed to polyvinylpyrrolidone coating, without nanoparticles), three low-dose tanks (G-I: seaweed exposed to 0.1 mg L^{-1} of PVP-AgNPs), and three high dose tanks (J-L: seaweed exposed to 1.0 mg L^{-1} of PVP-AgNPs) were employed. Three replicate samples were taken from each tank every 7 days, resulting in 180 samples per trial managed.

Each seaweed was washed with ultrapure water to remove salts and contaminants from seawater. The manually homogenized algae were subjected to acid digestion with microwave energy for total Ag determination by ICP-MS, and to an enzymatic extraction for AgNPs content determination by SP-ICP-MS.

2.4. Total Ag determination by ICP-MS after microwave-assisted acid digestion

Microwave-assisted acid digestion was used for sample preparation before total Ag determination by ICP-MS. A mass of 1.0000 g of crushed and homogenized sample was introduced in the Teflon vessels of the microwave lab station described in section 2.1. The samples were mixed with 3 mL of 69% HNO_3 (w/v), 1 mL of 33% H_2O_2 (w/v) and 4 mL of ultrapure water. The MW program consisted of four steps at 800W of MW energy: 1) From room temperature to $90 \text{ }^\circ\text{C}$ in 4 min. 2) From 90 to $140 \text{ }^\circ\text{C}$ in 5 min. 3) From 140 to $200 \text{ }^\circ\text{C}$ in 5 min. 4) Hold at $200 \text{ }^\circ\text{C}$ for 20 min.

Three seaweed replicates were taken from each tank and digested in triplicate, together with two blanks per set of digestions. Finally, the digests were diluted at 25 mL with ultrapure water before ICP-MS analysis.

The digested samples were analyzed by ICP-MS using the instrument described in section 2.1. and the operational conditions listed in Table 1 (a). Kinetic Energy Discrimination (KED) was used to avoid the polyatomic interferences in ICP-MS introducing a He flow rate of 4.5 mL min^{-1} in the collision cell. Furthermore, due to the matrix effect, standard addition calibrations were performed between 0 and $15.0 \mu\text{g L}^{-1}$ of Ag and using $5.0 \mu\text{g L}^{-1}$ of ^{103}Rh as an internal standard.

Table 1
Operational conditions for ICP-MS (a) and SP-ICP-MS (b).

(a) Operational conditions for ICP-MS	
Parameter/component	Type/mode/value
Nebulizer	Meinhard CR R ⁺
Nebulizer chamber	5 °C refrigerated glass cyclone chamber with Peltier PC ^{3X}
Cone material	Nickel/aluminum
Radiofrequency power	1600 W
Ar gas flow	15 L min ⁻¹ (Plasma) 1.15 L min ⁻¹ (Nebulizer) 1.2 L min ⁻¹ (Auxiliary)
Analyte	Ag
Operation mode	KED
He gas flow	4.5 mL min ⁻¹
Integration time	1000 ms
m/z	¹⁰⁷ Ag (¹⁰³ Rh as internal standard)
Replicates per sample	3
RPQ	0.2
(b) Operational conditions for SP-ICP-MS	
Operation mode	Standard
Sample flow rate	0.182–0.199 mL min ⁻¹
Acquisition time	100 s
Dwell time	50 μs
Number of readings	2,000,000
Transport efficiency	8.8–11.5%

2.5. AgNPs analysis by SP-ICP-MS after ultrasound-assisted enzymatic extraction

An ultrasound-assisted extraction with an enzymatic mixture (Macerozyme® R-10) was selected to separate PVP-AgNPs from the seaweed matrix, without primary size and AgNPs concentration changes. The methodology was previously developed and validated by López-Mayán et al. (2022). For the extraction, 0.0500 g of homogenized wet seaweed was weighed and mixed with a buffer of citric acid/sodium citrate (7 mL of 2/2 mM buffer, pH 4.5). The mixture was submitted to 2.5 min of 20% amplitude ultrasonication with an ultrasound probe working in pulse mode (1/1 s on/off). Then 25 g L⁻¹ of the enzyme mixture from *Rhizopus* sp. (hemicellulose, pectinase, and cellulase) was added. The enzymatic extracts were incubated for 6 h in a Boxcult temperature-controlled incubation chamber at 37 °C and 150 rpm. The enzymatic extracts with solid remains of seaweed were filtered with 5 μm cellulose syringe filters. Two blanks were prepared for each set of operational conditions or day of analysis. Finally, the extracts were diluted with 1% (v/v) glycerol before SP-ICP-MS analysis.

The diluted extracts were analyzed by ICP-MS working in Single-Particle (SP-ICP-MS) mode. The operational conditions of SP-ICP-MS are listed in Table 1(b). Syngistix™ Nano Application software requires the measurements of the sample flow rate and the transport efficiency (TE%) before sample analysis. The sample flow rate was calculated by aspirating ultrapure water through the peristaltic pump for 1 min (in triplicate) and measuring the mass. The transport efficiency was calculated by the software after measuring the signals for an ionic Au calibration (0–3.0 μg L⁻¹) and the Au nanospheres reference material of 49.6 nm in size at a concentration of 9.89 × 10⁴ particles mL⁻¹. For individualized nanoparticle detection, it was necessary to reduce the acquisition time to the order of μs-ms and a large dilution of the samples (100–350 times) to avoid the matrix effect; then, the SP-ICP-MS measurements were performed using an external Ag ionic calibration between 0 and 5.0 μg L⁻¹ prepared in ultrapure water. Finally, the AgNPs concentration and size distributions in the diluted extracts were obtained directly from the software after analysis, and they were used to calculate the concentrations in the seaweed samples.

2.6. Analysis of AgNPs in the enzymatic extracts by electron microscopy

The nanoparticles present in seaweed enzymatic extracts of *Palmaria palmata* and *Ulva* sp., both exposed to 1.0 mg L⁻¹ of AgNPs, were

characterized by transmission electron microscopy (TEM) and scanning transmission electron microscopy (STEM). For this purpose, the extracts were previously subjected to a cleaning and purification process to remove organic matter. The cleaning procedure consisted of filtration by ultracentrifugation using Amicon® Ultra 30 KDa centrifugal filter units. The filters were filled up with 0.5 mL of the extracts and centrifugated to 14,000 g at 4 °C for 20 min. The process was repeated five times adding 0.5 mL of ultrapure water. Finally, 0.5 mL of absolute ethanol was added to the extract and shaken to remove the organic matter excess. The preconcentrated and cleaned seaweed extracts (25 μL) were collected and 5 drops of 3 μL were added dropwise to the microscopy Ti grid, dried at room temperature and inserted in the STEM holder.

The image processing software ImageJ (developed by W. Rasband, National Institutes of Health and the Laboratory for Optical and Computational Instrumentation, Bethesda, Maryland, USA) was used to measure the AgNPs sizes by TEM.

2.7. Statistical analysis

Statgraphics XVIII (Warrenton, USA) was used for the statistical analysis in this research work. One-way ANOVA tests were performed to compare if there were significant differences over time for the concentrations of total Ag and AgNPs in control, solvent, 0.1 mg L⁻¹ and 1.0 mg L⁻¹ of PVP-AgNPs exposure tanks.

3. Results and discussion

3.1. Total Ag determination in seaweed exposed to AgNPs by ICP-MS

Total Ag contents (ionic Ag and Ag as AgNPs) in *Palmaria palmata* and *Ulva* sp. were determined by ICP-MS following the methodology described in section 2.4. The digested samples were diluted 25 and 50 times before ICP-MS analysis. The analytical performance of the methodology for total Ag determination was also assessed. The Limit of Detection (LOD) and Limit of Quantification (LOQ) were calculated using the 3σ/slope and 10σ/slope criteria, respectively (where σ is the standard deviation of the blank, that was divided by the slope of the standard addition calibration graph). The isotope ¹⁰⁷Ag was selected due to its higher relative abundance and the lower limit of detection; the LOD and LOQ obtained were 2.2 and 7.7 ng g⁻¹, respectively. The accuracy was evaluated through the analytical recovery due to a lack of reference materials. The mean analytical recovery percentage was 101 ± 3%. Furthermore, the precision was evaluated through repeatability (n = 5) with correlation coefficients lower than 5%.

3.1.1. Variation of total Ag content in *Palmaria palmata*

The concentration of total Ag was determined in red algae (*Palmaria palmata*) exposed to different concentrations (0.1 and 1.0 mg L⁻¹) of AgNPs. Fig. 1(a) shows the concentration of Ag in *Palmaria palmata* grown in control and solvent tanks for 28 days (concentration as mean ± standard deviation of the values measured for each group of tanks). The seaweed cultured in control tanks (A-C) and tanks exposed to the nanoparticle coating of PVP (D-F) did not present bioaccumulation of Ag. These basal Ag concentrations were lower than 0.02 μg g⁻¹ w.w. (wet weight). The one-way ANOVA test performed showed for control and solvent tanks P-values greater than 0.05; then, this confirms that there were no statistically significant differences between the averages at the different sampling days at a 95 % of significance level. Fig. 1(b) shows total Ag concentration in *Palmaria palmata* in control, solvent, low (G-I), and high (J-L) exposure dose tanks for 28 days. *Palmaria palmata* exposed to 0.1 mg L⁻¹ of AgNPs showed bioaccumulation of total Ag with exposure time until 21 days when the highest concentration of 0.52 ± 0.04 μg g⁻¹ w.w. was reached. Significant differences were found in Ag concentration with exposure time at a 95% of confidence level. The multiple range test showed a linear increase until 21 days and then the concentration remains practically constant. In the case of the seaweed

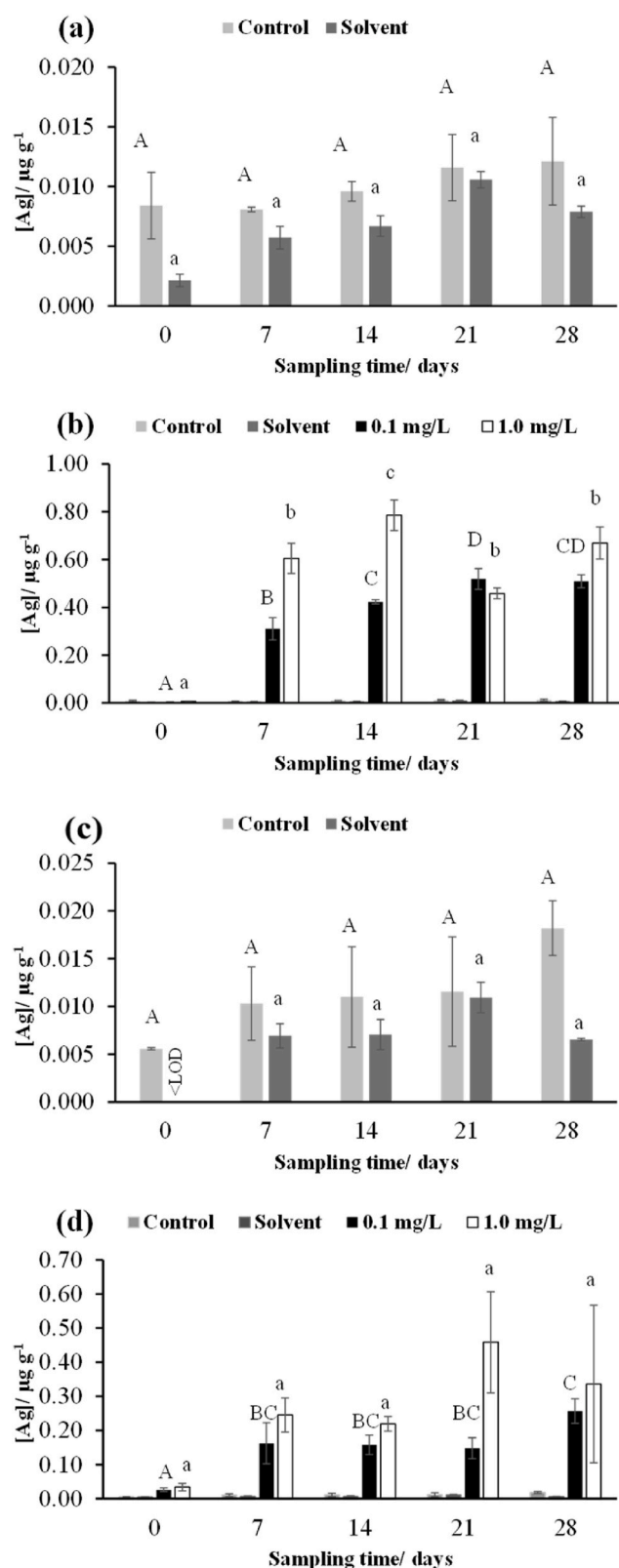


Fig. 1. Total Ag bioaccumulation: (a) control and solvent in *Palmaria palmata*; (b) control, solvent, 0.1, and 1.0 mg L⁻¹ in *Palmaria palmata*; (c) control and solvent in *Ulva sp.*; and (d) control, solvent, 0.1, and 1.0 mg L⁻¹ in *Ulva sp.* for 28 days. Error bars represent the standard deviation of the values measured for each group of tanks. Different letters indicate significant differences (one-way ANOVA, P -value < 0.05) between sampling times for each exposure dose (uppercase for control and 0.1 mg L⁻¹ tanks, and lowercase for solvent and 1.0 mg L⁻¹ tanks).

exposed to 1.0 mg L⁻¹, bioaccumulation is not proportional to the exposure dose and the highest concentration reached $0.79 \pm 0.06 \mu\text{g g}^{-1}$ w.w. at 14 days after exposure. The multiple range test also showed the linear increase of the concentration until reaching a maximum at 14 days after exposure, followed by a concentration decrease. Not significant differences were found between the concentrations measured at days 7, 21 and 28.

Table S.1. (supplementary electronic information) summarizes the concentrations of total Ag measured at days 0 and 28 after exposure in *Palmaria palmata* for the control, solvent, low, and high exposure dose (0.1 mg L⁻¹ and 1.0 mg L⁻¹ of AgNPs, respectively) tanks, and Figure S.1. (supplementary electronic information) shows total Ag concentration in *Palmaria palmata* taken from all the different control tanks (tanks A-C, Figure S1(a)), the tanks exposed to the nanoparticle coating (tanks D-F, Figure S1(b)), the tanks exposed to 0.1 mg L⁻¹ of AgNPs (tanks G-I, Figure S1(c)), and the tanks exposed to 1.0 mg L⁻¹ of AgNPs (tanks J-L, Figure S1(d)).

3.1.2. Variation of total Ag content in *Ulva sp.*

The concentration of total Ag was also determined in green seaweed (*Ulva sp.*) exposed to both concentrations of these NPs. Fig. 1(c) shows the concentration of total Ag in *Ulva sp.* from control and solvent tanks during the 28 days (concentration as mean \pm standard deviation of the values measured for each group of tanks). As in *Palmaria palmata*, the control tanks and the tanks exposed to PVP did not show bioaccumulation, with basal Ag concentrations lower than $0.03 \mu\text{g g}^{-1}$ w.w. Besides, no significant differences were found for Ag concentration in the control and solvent tanks as a function of exposure time. Fig. 1(d) shows the bioaccumulation trend in *Ulva sp.* exposed to 0.1 and 1.0 mg L⁻¹ for 28 days. The *Ulva sp.* specimens exposed to a concentration of 0.1 mg L⁻¹ showed lower bioaccumulation than *Palmaria palmata*. The highest mean concentration measured was $0.26 \pm 0.04 \mu\text{g g}^{-1}$ w.w., reached 28 days after exposure. Significant differences were observed between total Ag concentrations as a function of exposure days. The concentration increased until 7 days and then remained practically constant with the exposure time, reaching the highest mean concentration at 28 exposure days. The bioaccumulation was slightly higher in seaweeds exposed to 1 mg L⁻¹, reaching the maximum concentration of $0.46 \pm 0.15 \mu\text{g g}^{-1}$ w.w. at day 21 of exposure. In this case, no statistically significant differences were found between Ag concentrations as a function of the exposure day. This finding could be due to the high variability of the concentrations observed for seaweed from the different tanks on days 21 and 28 after exposure. Table S1 also summarizes the concentrations of Ag in *Ulva sp.* from the control, solvent, low and high exposure dose (0.1 mg L⁻¹ and 1.0 mg L⁻¹ of PVP-AgNPs) tanks at days 0 and 28 of exposure. Figure S.2. shows the concentration of Ag in *Ulva sp.* samples extracted from the different control tanks (tanks A-C, Figure S2(a)), the tanks exposed to the PVP nanoparticle coating (tanks D-F, Figure S2(b)), the tanks exposed to 0.1 mg L⁻¹ of PVP-AgNPs (tanks G-I, Figure S2(c)), and the tanks exposed to 1.0 mg L⁻¹ of PVP-AgNPs (tanks J-L, Figure S2(d)).

3.2. AgNPs determination in seaweed exposed to AgNPs by SP-ICP-MS

The AgNPs content in *Palmaria palmata* and *Ulva sp.* was determined by ICP-MS working in SP-ICP-MS mode following the methodology described in section 2.5. A solution of 1% (v/v) glycerol was used to dilute the seaweed extracts from 100 to 350 times. The experimental flow rates and transport efficiencies were between 0.182 and 0.199 mL min⁻¹ and 8.8–11.5%, respectively. The analytical performance was also studied for SP-ICP-MS. The sensitivity was evaluated through the limit of detection in size (LOD_{size}) and particle number (LOD_{number}) using Laborda et al. (2020) criteria. A blank submitted to the whole extraction procedure and diluted 100 times in 1% (v/v) glycerol was used to calculate the limits of detection. The LOD_{size} resulted in 14 and 12 nm using the 5 σ and 3 σ criteria, respectively (the 5 σ criteria was

selected to avoid false positives). The LOD_{number} were 2.40×10^6 part L^{-1} (instrumental limit) and 4.34×10^7 part g^{-1} (referred to the wet seaweed sample). The precision of the methodology was evaluated through the study of the repeatability in the analysis of *Palmaria palmata* and *Ulva* sp. extracts submitted to the enzymatic extraction; the measurements ($n = 5$) of the most frequent sizes, mean sizes and AgNPs concentration reported variation coefficients lower than 18%. Furthermore, the accuracy of the extraction method was guaranteed, with mean analytical recoveries of $112 \pm 12\%$ ($n = 3$) at a concentration level of 6.0×10^7 part mL^{-1} . The stability of the AgNPs during the extraction procedure from exposed *Palmaria palmata* and *Ulva* sp. was tested in a previous study of the research group by SP-ICP-MS and transmission electron microscopy (López-Mayán et al., 2022).

3.2.1. AgNPs content and size distribution in *Palmaria palmata*

The AgNPs content and their size distributions were studied in *Palmaria palmata* after ultrasound-assisted enzymatic extraction. Since the total Ag content in the control tanks corresponded to the basal content, only the algae samples exposed to AgNPs were studied by SP-ICP-MS.

Fig. 2(a) and (b) show the average intertank nanoparticle concentrations of *Palmaria palmata* exposed to concentrations of 0.1 mg L^{-1} (average of Tanks G, H, and I) and 1.0 mg L^{-1} (average of tanks J, K, L) for 28 days, respectively. Statistical differences were found in the AgNPs concentrations with exposure time at 0.1 mg L^{-1} . The AgNPs concentration increased with the exposure time until $7.14 \times 10^8 \pm 2.38 \times 10^8$ part g^{-1} w.w. at 28 days. The multiple range test also showed the statistical differences between concentrations between 7 and 28 days, and between 14 and 28 days. Furthermore, Fig. 2(c) shows the most frequent and mean sizes in the case of *Palmaria palmata* exposed to a concentration of 0.1 mg L^{-1} for 28 days. The most frequent and mean sizes were between $18 \pm 2 \text{ nm}$ (7 days) and $19 \pm 1 \text{ nm}$ (28 days), and between $22 \pm 2 \text{ nm}$ (7 days) and $23 \pm 1 \text{ nm}$ (28 days), respectively. As expected, higher AgNPs concentrations were found in red seaweed exposed to 1.0 mg L^{-1} showing statistical differences between the concentrations measured on different days. The concentration increased until $1.63 \times 10^9 \pm 5.47 \times 10^8$ part g^{-1} w.w. at day 14, and after that, the mean concentration decreased. Fig. 2(d) shows the most frequent and mean sizes in the case of *Palmaria palmata* exposed to 1.0 mg L^{-1} of PVP-AgNPs for 28 days. The most frequent and mean sizes were between $21 \pm 1 \text{ nm}$ (7 days) and $19 \pm 4 \text{ nm}$ (28 days), and between $30 \pm 3 \text{ nm}$ (7 days) and $24 \pm 1 \text{ nm}$ (28 days), respectively.

Finally, Fig. 3 shows two examples of the size distribution histograms obtained for the enzymatic extracts of *Palmaria palmata* exposed to both concentrations of AgNPs.

3.2.2. AgNPs content and size distribution in *Ulva* sp.

The AgNPs content and their size distributions were studied in the enzymatic extracts of *Ulva* sp. samples exposed to AgNPs. Fig. 4 shows the average intertank concentrations (a, b) and the most frequent and mean sizes (c, d) of those NPs in the samples.

The analysis of the results obtained showed statistical differences between the AgNPs concentrations for *Ulva* sp. exposed to 0.1 mg L^{-1} on different days. The AgNPs content increased with the exposure time until $1.19 \times 10^9 \pm 2.81 \times 10^8$ part g^{-1} w.w. at day 28. As expected, the higher nanoparticle concentration was measured for algae exposed to 1.0 mg L^{-1} , reaching a value of $3.23 \times 10^9 \pm 2.34 \times 10^7$ part g^{-1} w.w. at 28 exposure days. Furthermore, Fig. 4(c, d) show the most frequent sizes and mean sizes for both seaweeds exposed to both concentrations of NPs. The most frequent sizes were approximately 21 nm for both types of seaweed and the mean sizes were around 31 nm.

Two examples of size distribution histograms obtained for the enzymatic extracts of *Ulva* sp. seaweeds exposed to NPs concentrations of 0.1 and 1.0 mg L^{-1} are shown in Fig. 3(c) and (d), respectively.

The presence of Ag in the environment deserves to be studied because of its elevated toxicity to marine organisms including seaweed. Lee et al. (2020) developed a semi-automated toxicity test based on the

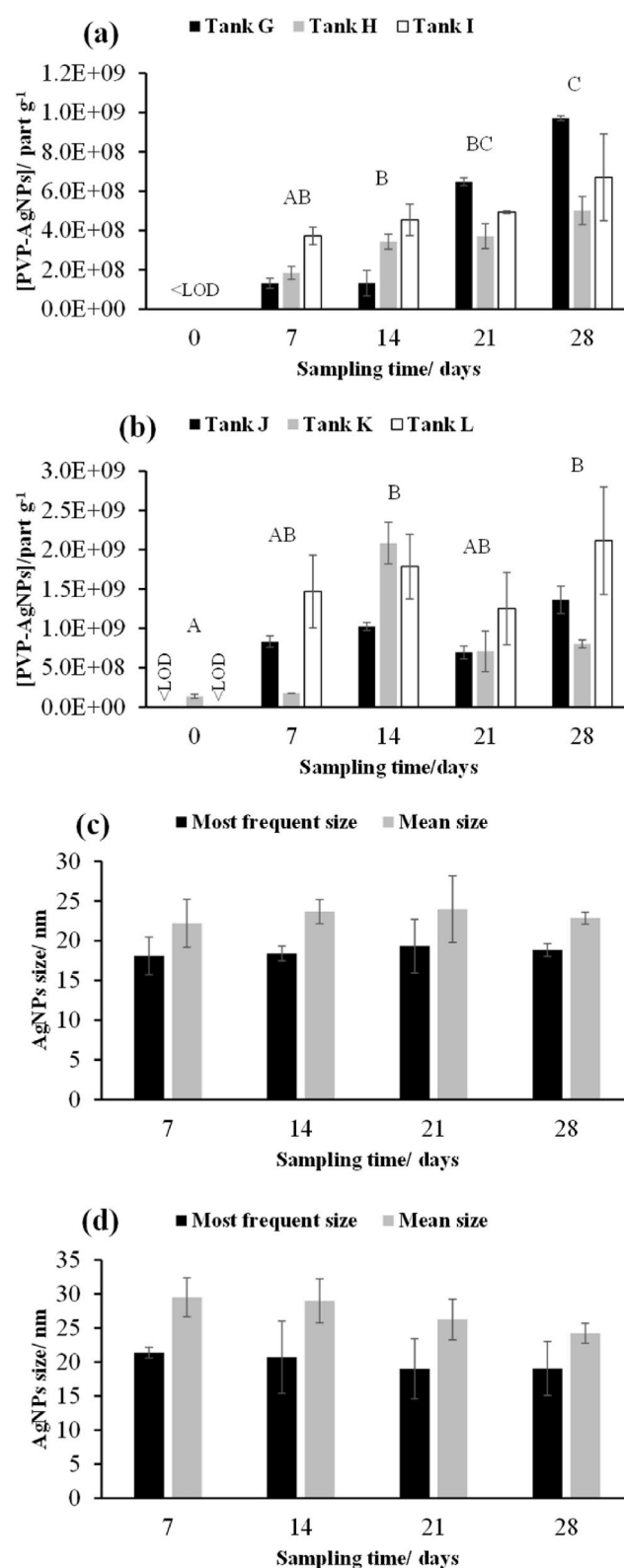


Fig. 2. AgNPs content in *Palmaria palmata* exposed to (a) 0.1 mg L^{-1} and (b) 1.0 mg L^{-1} of PVP-AgNPs, and most frequent and mean sizes exposed to (c) 0.1 mg L^{-1} and (d) 1.0 mg L^{-1} . Error bars represent the standard deviation of the values measured for each seaweed sample ($n = 3$) (a and b), and the standard deviation of the values measured for each group of tanks (c and d). Different letters indicate significant differences (one-way ANOVA, P -value < 0.05) between tank means at different sampling times for each exposure dose.

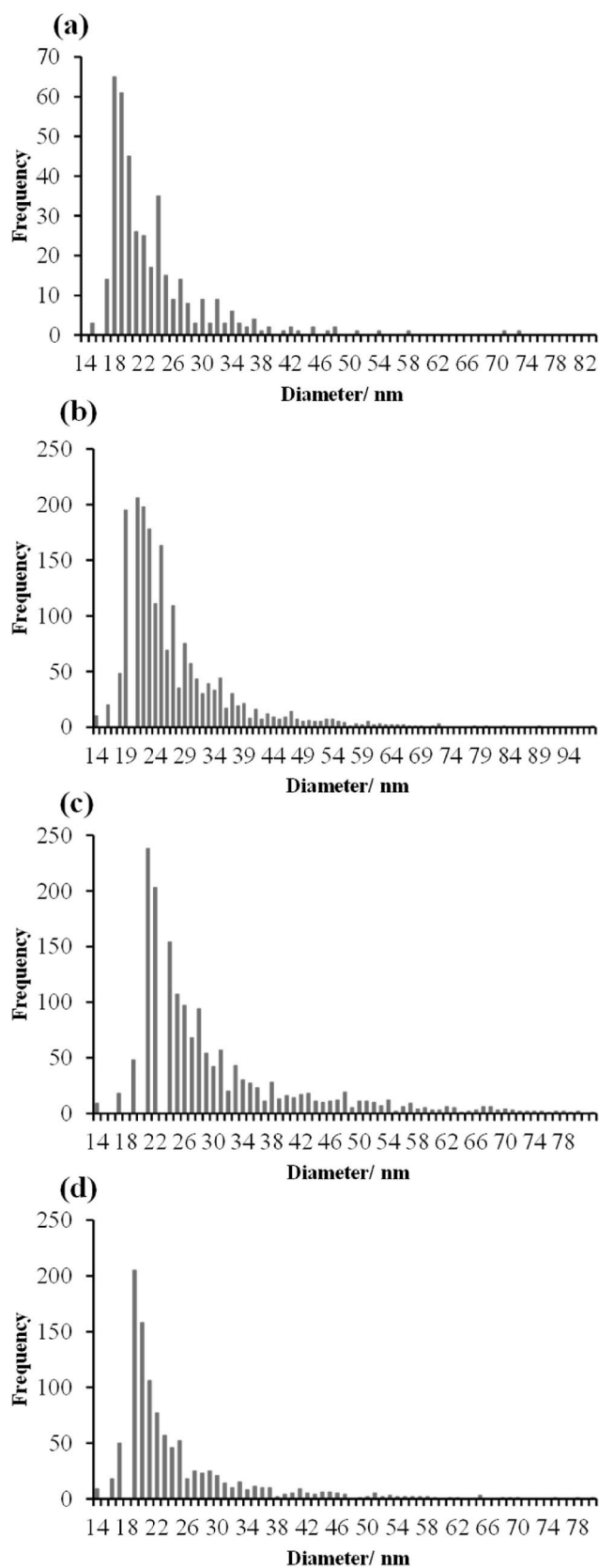


Fig. 3. Size distribution histograms of PVP-AgNPs corresponding to extracts of *Palmaria palmata* exposed to (a) 0.1 mg L⁻¹ and (b) 1.0 mg L⁻¹, and *Ulva* sp. exposed to (c) 0.1 mg L⁻¹ and (d) 1.0 mg L⁻¹ of PVP-AgNPs.

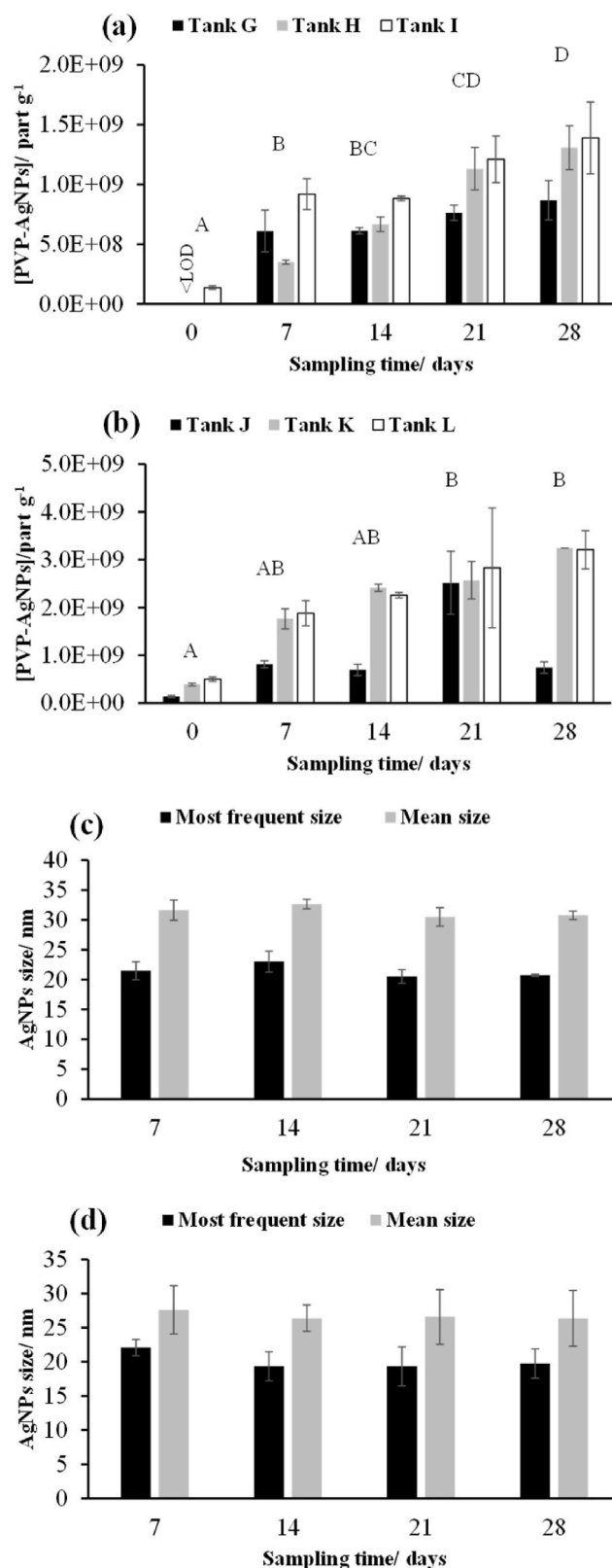


Fig. 4. AgNPs content in *Ulva* sp. exposed to (a) 0.1 mg L⁻¹ and (b) 1.0 mg L⁻¹ of PVP-AgNPs, and most frequent and mean sizes exposed to (c) 0.1 mg L⁻¹ and (d) 1.0 mg L⁻¹. Error bars represent the standard deviation of the values measured for each seaweed sample (n = 3) (a and b), and the standard deviation of the values measured for each group of tanks (c and d). Different letters indicate significant differences (one-way ANOVA, P-value < 0.05) between tank means at different sampling times for each exposure dose.

measurement of the inhibition of reproduction of *Ulva pertusa* by different compounds (Ag, As, phenol, herbicides, volatile organic compounds, antifouling agents) after 96 h of exposure. The half maximal effective concentration (EC50) for Ag was 0.132 mg L^{-1} , a value between those obtained for the most toxic compounds (the antifouling agent Irgarol with an $\text{EC}_{50} = 0.048 \text{ mg L}^{-1}$, and As with an $\text{EC}_{50} = 0.172 \text{ mg L}^{-1}$). In a previous study, (Siddiqui and Bielmyer-Fraser, 2019) compared the accumulation of AgNO_3 and silver oxide nanoparticles (AgONPs) ranging in size from 40 to 70 nm in two seaweed species (*Ulva lactuca* and *Agardhiella subulata*), finding that the accumulation was species-dependent. Seaweeds were exposed together to test solutions of 0, 10, 100 and $1000 \text{ } \mu\text{g L}^{-1}$ prepared in synthetic seawater (salinity 30 ppt) in 2-L culture dishes for a maximum of 48 h. The green algae *Ulva lactuca* showed more accumulation at 24 h after exposure to 100 and $1000 \text{ } \mu\text{g L}^{-1}$ AgNO_3 and $1000 \text{ } \mu\text{g L}^{-1}$ AgONPs, followed by a decrease in the concentration of Ag in the tissue at 48 h. However, the concentration of Ag in red algae *A. subulata* increased at 48 h after exposure to AgNO_3 . The authors concluded that: 1) *U. lactuca* regulated Ag tissue concentration better than *A. subulata*; 2) the accumulation of AgONPs (40–70 nm in size) was better regulated or they were less available than ionic Ag. *U. lactuca* exposed to $10\text{--}1000 \text{ } \mu\text{g L}^{-1}$ of AgNO_3 or AgONPs accumulated approximately $7\text{--}150 \text{ } \mu\text{g g}^{-1}$ d.w. and $5\text{--}100 \text{ } \mu\text{g g}^{-1}$ d.w., respectively. Those concentrations were similar to those measured by Turner et al. (2012) with ranges of approximately $30\text{--}110 \text{ } \mu\text{g g}^{-1}$ and $5\text{--}30 \text{ } \mu\text{g g}^{-1}$ d.w., after the exposure of *U. lactuca* to nominal concentrations between 0 and $100 \text{ } \mu\text{g L}^{-1}$ of AgNO_3 or AgNPs ($58 \pm 27 \text{ nm}$), respectively, for 48 h. Experiments were carried out by exposing two discs of *Ulva lactuca* (each disc made of a 6 mg d.w. portion taken from the central portion of thalli) in 100 mL of seawater; the PET beakers were lidded and placed on an orbital shaker at 100 rpm. These authors reported a dose-response for AgNPs similar to that observed for ionic Ag at much lower concentrations, suggesting that the toxicity of AgNPs is related to their dissolution rate in aquatic media. Sfriso et al. (2019) studied the effects of short-time exposure of *Ulva rigida* C. Agardh seaweed to citrate-coated AgNPs ($35 \pm 9 \text{ nm}$ in size) and AgNO_3 in artificial seawater for 24 h. Flasks of 100 mL with 500 mg of fresh seaweed thalli were used for the tests. The accumulation of Ag followed a Langmuir isotherm with a saturation point of $11.3 \text{ } \mu\text{g Ag g}^{-1}$ w.w. from a 5 mg L^{-1} solution of AgNPs. The uptake of the element was very fast, with Ag reaching concentrations in the seaweed of $8.50 \text{ } \mu\text{g g}^{-1}$ w.w. after exposure to 1 mg L^{-1} of AgNPs for 24 h. These authors suggest that the toxicity of Ag on seaweed should be reduced by the presence of inorganic and organic ligands concentrations in real marine transitional environments. The differences in accumulation can be explained according to the diverse behavior of species, different sizes and coatings of the nanoparticles tested in the experiments. Zhang et al. (2020) reported that the type of coating and surface charge of AgNPs influences the bioaccumulation dynamics in freshwater algae (*Chlorella vulgaris*). The algae surface cells are a negatively charged plasma membrane, with negatively charged groups. Therefore, polyethylene-coated AgNPs (positively charged) and citrate-coated AgNPs (negatively charged) experienced electrostatic attraction and repulsion with the algal membrane, respectively.

The sizes of the nanoparticles used in the present study (15 nm, with a PVP coating, negatively charged) were smaller than those used in previous studies with seaweed, and therefore, they are expected to have more industrial applications as bactericides. It has been demonstrated that the antibacterial effect increases with lowering particle size and could be explained due to the increased number concentration of particles (Agnihotri et al., 2014). The maximum concentrations of total Ag measured in the present study were: $0.52 \pm 0.04 \text{ } \mu\text{g g}^{-1}$ w.w. (at day 21, exposure to 0.1 mg L^{-1} of PVP-AgNPs) and $0.79 \pm 0.06 \text{ } \mu\text{g g}^{-1}$ w.w. (at day 14, 1.0 mg L^{-1}) in *Palmaria palmata*, and $0.26 \pm 0.04 \text{ } \mu\text{g g}^{-1}$ w.w. (at day 28, 0.1 mg L^{-1}) and $0.46 \pm 0.15 \text{ } \mu\text{g g}^{-1}$ (at day 21, 1.0 mg L^{-1}) in *Ulva* sp. *Palmaria palmata* reached the maximum concentration faster than *Ulva* sp. Concentration in seaweed does not rise in equal proportion

to the concentration of exposure; thus, it can be observed that increasing ten times the exposure concentration implies an increase of 1.5 and 1.8 times the content of Ag in *Palmaria palmata* and *Ulva* sp., respectively. The percentage of humidity of *Palmaria* and *Ulva* is approximately 90%. Therefore, the concentrations of Ag determined in the present work were smaller than those found in previous studies, probably because seaweeds were exposed to nanoparticles mixed with growing media and the phytoplankton that was used for feeding. It was expected that the accumulation of Ag would be reduced in the presence of organic matter in marine media. Thus, Xiang et al., 2018 reported the toxicity of AgNPs in freshwater green algae (*Microcystis aeruginosa*), where AgNPs adhesion, penetration and changes in the cell membranes decreased with the organic matter present, due to the dissolved Ag ratio decrease. Sfriso et al. (2019) also reported that inorganic and organic ligands diminished the toxicity of algae up to concentrations of 0.5 ppm of silver nanoparticles in transitional waters where most primary producers are grown. In our study, no morphological changes in seaweed tissues were observed by TEM analysis after exposure to a maximum dose of 1.0 mg L^{-1} . No evident difference in the structural organization of the cells was observed between control and exposed samples of both types of seaweed after 0 and 28 days. These observations indicate that seaweed was not damaged or significantly disturbed by the exposure conditions. The variation of metal concentrations (As, Cd, Co, Cr, Cu, Mo, Ni, Pb, Rb, Sb, Se, V and Zn) was also evaluated in the acid digests of both exposed seaweed by ICP-MS. The following elements could not be quantified: As, Se, Sb, and Zn; and most of the other elements showed no significant concentration differences with exposure time and doses. Only the concentrations of Cd and Pb decreased from 0.013 to $0.006 \text{ } \mu\text{g g}^{-1}$ (day 0 and 28), and from 0.7 to $0.3 \text{ } \mu\text{g g}^{-1}$ (day 21), respectively, at the dose of 1 mg L^{-1} in *Palmaria Palmata*.

Moreover, tanks used for cultivation in the present investigation (40 L of seawater with addition of growth medium) were also much bigger than in other studies, and water was renewed periodically with addition of new nanoparticles, but it was not stirred like in the study by Turner et al. (2012). In this case, orbital stirring at 100 rpm under lab conditions could contribute to the accumulation of AgNPs in seaweed, and to the high concentrations of the element measured in that research.

The maximum concentrations of AgNPs were achieved at 14 days for *Palmaria palmata* ($1.63 \times 10^9 \pm 5.47 \times 10^8 \text{ part g}^{-1}$ w.w., 1.0 mg L^{-1}) and at 28 days for *Ulva* sp. ($3.23 \times 10^9 \pm 2.34 \times 10^7 \text{ part g}^{-1}$ w.w., 1.0 mg L^{-1}) with most frequent sizes of approximately 20 nm. The maximum concentration of AgNPs measured in *Ulva* sp. was higher than in *Palmaria palmata*, even when the total concentration of the element was smaller. This finding confirms again the different accumulation patterns observed for both species, representative of green and red seaweed. Then, this study contributes to increasing the knowledge about AgNPs in marine organisms after a longer-term exposure (28 days) to relatively small-size nanoparticles (15 nm) in a real marine growing media.

3.3. Characterization of AgNPs

The PVP-AgNPs were characterized in a previous study (Araújo et al., 2022). The size of the PVP-AgNPs in ultrapure water was characterized by TEM, where NPs were well-dispersed with a primary size of $24.0 \pm 0.5 \text{ nm}$. The AgNPs sizes were larger than those stated by the supplier, possibly due to the high dispersion and reactivity of silver.

This higher size than the theoretical 15 nm of PVP-AgNPs was also in agreement with the sizes found in the enzymatic extracts by SP-ICP-MS and TEM.

The enzymatic extracts of *Palmaria palmata* and *Ulva* sp. exposed to 1.0 mg L^{-1} of PVP-AgNPs were submitted to the preconcentration and cleaning process described in section 2.6., before their deposition in the Ti grid to visualize AgNPs using STEM. Fig. 5 shows the STEM micrographs for *Palmaria palmata* extracts working in TEM (Fig. 5(a)) and STEM mode (Fig. 5(b) and (c)), and for *Ulva* sp. extracts working in TEM

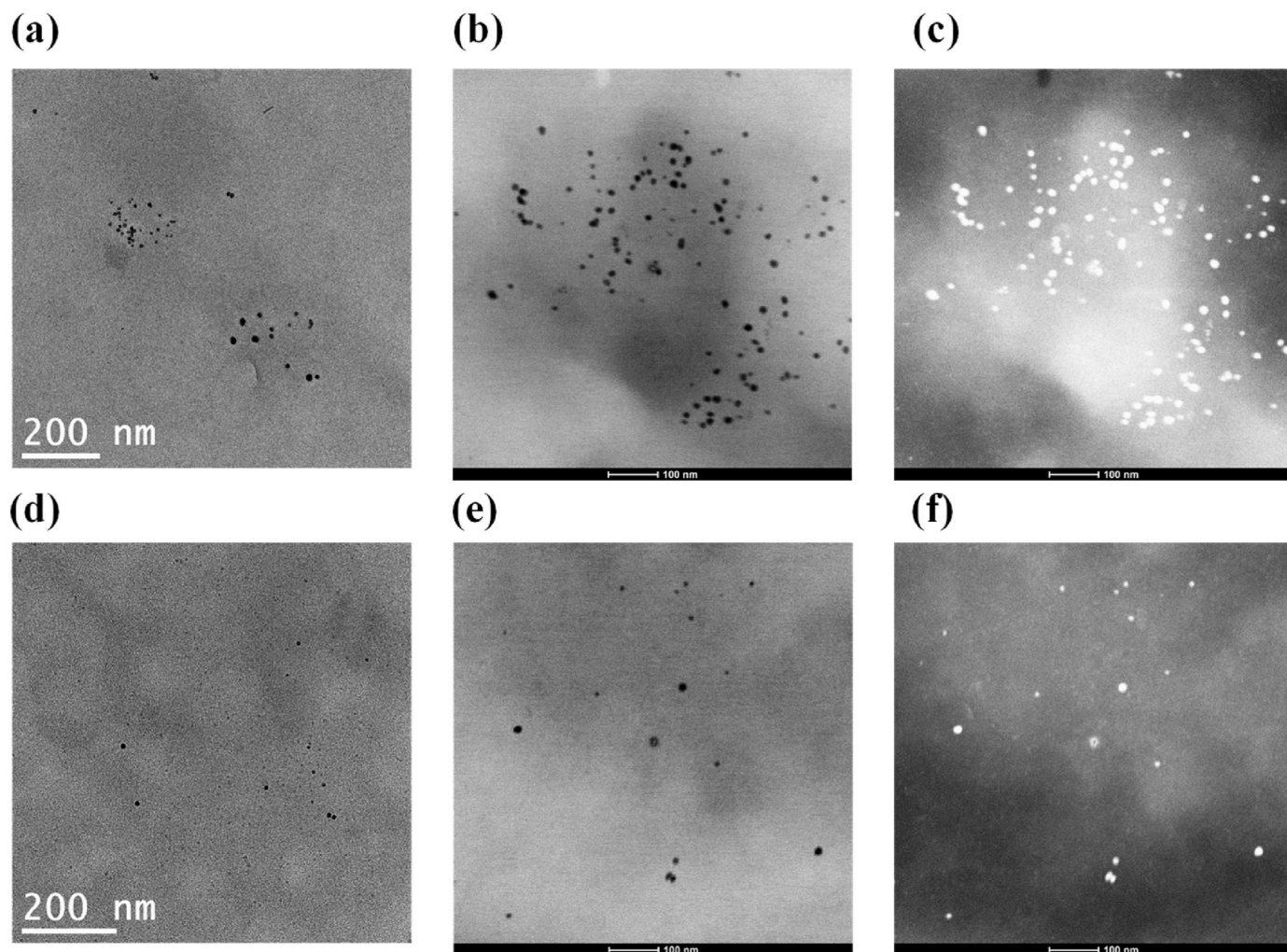


Fig. 5. Micrographs obtained by: (a) TEM, (b) STEM bright field, and (c) STEM High Angle Annular Dark Field of enzymatic extracts *Palmaria palmata* exposed to 1.0 mg L^{-1} of PVP-AgNPs; (d) TEM, (e) STEM bright field, and (f) STEM high angle annular dark field enzymatic extracts of *Ulva* sp. exposed to 1.0 mg L^{-1} of PVP-AgNPs.

(Fig. 5(d)) and STEM mode (Fig. 5(e) and (f)).

In both types of seaweed extracts, the TEM and STEM micrographs confirm the presence of spherical AgNPs. The mean sizes measured ($n = 200$) were 24 and 20 nm for *Palmaria palmata* and *Ulva* sp., respectively. The sizes found in the TEM micrographs agreed with the most frequent sizes obtained by SP-ICP-MS for *Palmaria palmata* (between 21 ± 1 – 19 ± 4 nm) and *Ulva* sp. (between 22 ± 1 and 20 ± 2 nm).

4. Conclusions

Seaweeds are known for their ability to bioaccumulate heavy metals and trace elements. However, little is known about the ability of marine macroalgae to bioaccumulate nanomaterials and nanoparticles. In comparison to other studies, we investigated the bioaccumulation patterns of seaweed exposed in marine growing media to AgNPs of small particle size (15 nm), typical in industrial applications due to their greater antibacterial activity, and for longer times of exposure (28 days). Both seaweed, *Palmaria palmata* and *Ulva* sp., bioaccumulated AgNPs at different rates, and the increase of total Ag and AgNPs was not proportional to the exposure concentration. The maximum concentration levels of Ag reported in this study were lower than those found in the literature for shorter exposure times (<48 h), and higher particle sizes (20–100 nm) and most of them using synthetic media under laboratory conditions.

There are no regulations on maximum permitted levels of

nanoparticle content in foods such as algae, so further studies about the toxicity and bioaccumulation by different seaweed species simulating real marine environment exposure are needed to estimate environmental concentrations in real scenarios and elucidate the extent to which algae may be safe for human consumption or other applications such as soil fertilizers.

CRediT authorship contribution statement

Juan José López-Mayán: Writing – original draft, Validation, Methodology, Investigation, Formal analysis, Data curation. **Blanca Álvarez-Fernández:** Formal analysis. **Elena Peña-Vázquez:** Writing – review & editing, Validation, Supervision, Methodology, Investigation, Data curation, Conceptualization. **María Carmen Barciela-Alonso:** Writing – review & editing, Validation, Supervision, Methodology, Investigation, Data curation, Conceptualization. **Antonio Moreda-Piñero:** Resources, Funding acquisition, Conceptualization. **Julie Maguire:** Resources. **Mick Mackey:** Resources. **Pilar Bermejo-Barra:** Resources, Funding acquisition, Conceptualization.

Declaration of competing interest

The authors declare that they have no known competing financial interest or personal relationships that could have appeared to influence the work reported in this paper.

Acknowledgements

The authors wish to thank the financial support of Ministerio de Economía y Competitividad (project INNOVANANO, reference RT 2018-099222-B-100), European Union (INTERREG Atlantic Area, project NANOCULTURE, reference EAPA590/2018), and Xunta de Galicia (Grupo de Referencia Competitiva, grant number ED431C.2022/29).

Appendix A. Supplementary data

Supplementary data to this article can be found online at <https://doi.org/10.1016/j.chemosphere.2024.143872>.

Data availability

Data will be made available on request.

References

- Agnihotri, S., Mukherji, Soumyo, Mukherji, Suparna, 2014. Size-controlled silver nanoparticles synthesized over the range 5–100 nm using the same protocol and their antibacterial efficacy. *RSC Adv.* 4, 3974–3983. <https://doi.org/10.1039/c3ra44507k>.
- Ali, A.Y.A., Idris, A.M., Eltayeb, M.A.H., El-Zahhar, A.A., Ashraf, I.M., 2021. Bioaccumulation and health risk assessment of toxic metals in red algae in Sudanese Red Sea coast. *Toxin Rev.* 40, 1327–1337. <https://doi.org/10.1080/15569543.2019.1697886>.
- Ammar, E.E., Aioub, A.A.A., Elesawy, A.E., Karkour, A.M., Mouhamed, M.S., Amer, A.A. El-Shershaby, Nouran, A., 2022. Algae as bio-fertilizers: between current situation and future prospective. *Saudi J. Biol. Sci.* 29, 3083–3096. <https://doi.org/10.1016/j.sjbs.2022.03.020>.
- Araújo, M.J., Sousa, M.L., Fonseca, E., Felpeto, A.B., Martins, J.C., Vázquez, M., Mallo, N., Rodríguez-Lorenzo, L., Quarato, M., Pinheiro, I., Turkina, M.V., López-Mayán, J.J., Peña-Vázquez, E., Barciela-Alonso, M.C., Spuch-Calvar, M., Oliveira, M., Bermejo-Barrera, P., Cabaleiro, S., Espiña, B., Vasconcelos, V., Campos, A., 2022. Proteomics reveals multiple effects of titanium dioxide and silver nanoparticles in the metabolism of turbot, *Scophthalmus maximus*. *Chemosphere* 308, 136100. <https://doi.org/10.1016/j.chemosphere.2022.136110>.
- Arienza, M., Ferrara, L., 2022. Environmental fate of metal nanoparticles in estuarine environments. *Water* 14, 1297. <https://doi.org/10.3390/w14081297>.
- Asharani, P.V., Lian Wu, Y., Gong, Z., Valiyaveetil, S., 2008. Toxicity of silver nanoparticles in zebrafish models. *Nanotechnology* 19, 255102. <https://doi.org/10.1088/0957-4484/19/25/255102>.
- Banerjee, A., Roychoudhury, A., 2019. Nanoparticle-induced ecotoxicological risks in aquatic environments: concepts and controversies, *Nanomaterials in Plants. Algae and Microorganisms: Concepts and Controversies* 2, 129–141. <https://doi.org/10.1016/B978-0-12-811488-9.00007-X>.
- Bonanno, G., Orlando-Bonaca, M., 2018. Trace elements in Mediterranean seagrasses and macroalgae. A review. *Sci. Total Environ.* 618, 1152–1159. <https://doi.org/10.1016/j.scitotenv.2017.09.192>.
- Chae, Y., An, Y.J., 2016. Toxicity and transfer of polyvinylpyrrolidone-coated silver nanowires in an aquatic food chain consisting of algae, water fleas, and zebrafish. *Aquat. Toxicol.* 173, 94–104. <https://doi.org/10.1016/j.aquatox.2016.01.011>.
- Chernousova, S., Epple, M., 2013. Silver as antibacterial agent ion, nanoparticle, and metal. *Angew. Chemie - Int. Ed.* 52, 1636–1653. <https://doi.org/10.1002/anie.201205923>.
- Choi, O., Hu, Z., 2008. Size dependent and reactive oxygen species related nanosilver toxicity to nitrifying bacteria. *Environ. Sci. Technol.* 42, 4583–4588. <https://doi.org/10.1021/es703238h>.
- Cofrades, S., López-Lopez, I., Bravo, L., Ruiz-Capillas, C., Bastida, S., Larrea, M.T., Jiménez-Colmenero, F., 2010. Nutritional and antioxidant properties of different brown and red Spanish edible seaweeds. *Food Sci. Technol. Int.* 16, 361–370. <https://doi.org/10.1177/1082013210367049>.
- Gómez-Ordóñez, E., Jiménez-Escrig, A., Rupérez, P., 2010. Dietary fibre and physicochemical properties of several edible seaweeds from the northwestern Spanish coast. *Food Res. Int.* 43, 2289–2294. <https://doi.org/10.1016/j.foodres.2010.08.005>.
- Gubbins, E.J., Batty, L.C., Lead, J.R., 2011. Phytotoxicity of silver nanoparticles to *Lemma minor* L. *Environ. Pollut.* 159, 1551–1559. <https://doi.org/10.1016/j.envpol.2011.03.002>.
- Hwang, E.T., Lee, J.H., Chae, Y.J., Kim, Y.S., Kim, B.C., Sang, B.I., Gu, M.B., 2008. Analysis of the toxic mode of action of silver nanoparticles using stress-specific bioluminescent bacteria. *Small* 4, 746–750. <https://doi.org/10.1002/sml.200700954>.
- Książek, M., Asztemborska, M., Stęborowski, R., Bystrzejewska-Piotrowska, G., 2015. Toxic effect of silver and platinum nanoparticles toward the freshwater microalga *Pseudokirchneriella subcapitata*. *Bull. Environ. Contam. Toxicol.* 94, 554–558. <https://doi.org/10.1007/s00128-015-1505-9>.
- Laborda, F., Gimenez-Ingalaturre, A.C., Bolea, E., Castillo, J.R., 2020. About detectability and limits of detection in single particle inductively coupled plasma mass spectrometry. *Spectrochim. Acta Part B At. Spectrosc.* 169, 105883. <https://doi.org/10.1016/j.sab.2020.105883>.
- Lee, H., Park, J., Shin, K., Depuydt, S., Choi, S., De Saeger, J., Han, T., 2020. Application of a programmed semi-automated *Ulva pertusa* bioassay for testing single toxicants and stream water quality. *Aquat. Toxicol.* 221, 105426. <https://doi.org/10.1016/j.aquatox.2020.105426>.
- Lekamge, S., Miranda, A.F., Abraham, A., Ball, A.S., Shukla, R., Nugegoda, D., 2020. The toxicity of coated silver nanoparticles to the alga *Raphidocelis subcapitata*. *SN Appl. Sci.* 2, 1–20. <https://doi.org/10.1007/s42452-020-2430-z>.
- Levard, C., Hotze, E.M., Lowry, G.V., Brown, G.E., 2012. Environmental transformations of silver nanoparticles: impact on stability and toxicity. *Environ. Sci. Technol.* 46, 6900–6914. <https://doi.org/10.1021/es2037405>.
- Liao, C., Li, Y., Tjong, S.C., 2019. Bactericidal and cytotoxic properties of silver nanoparticles. *Int. J. Mol. Sci.* 20 (2), 449. <https://doi.org/10.3390/ijms20020449>.
- López-Mayán, J.J., Álvarez-Fernández, B., Peña-Vázquez, E., Barciela-Alonso, M.C., Moreda-Piñero, A., Bermejo-Barrera, P., 2022. Ultrasonication followed by enzymatic hydrolysis as a sample pre-treatment for the determination of Ag nanoparticles in edible seaweed by SP-ICP-MS. *Talanta* 247, 123556. <https://doi.org/10.1016/j.talanta.2022.123556>.
- Lu, W., Senapati, D., Wang, S., Tovmachenko, O., Singh, A.K., Yu, H., Ray, P.C., 2010. Effect of surface coating on the toxicity of silver nanomaterials on human skin keratinocytes. *Chem. Phys. Lett.* 487, 92–96. <https://doi.org/10.1016/j.cplett.2010.01.027>.
- McTeer, J., Dean, A.P., White, K.N., Pittman, J.K., 2014. Bioaccumulation of silver nanoparticles into *Daphnia magna* from a freshwater algal diet and the impact of phosphate availability. *Nanotoxicology* 8, 305–316. <https://doi.org/10.3109/17435390.2013.778346>.
- Navarro, E., Baun, A., Behra, R., Hartmann, N.B., Filser, J., Miao, A.J., Quigg, A., Santschi, P.H., Sigg, L., 2008. Environmental behavior and ecotoxicity of engineered nanoparticles to algae, plants, and fungi. *Ecotoxicology* 17, 372–386. <https://doi.org/10.1007/s10646-008-0214-0>.
- Pei, B., Zhang, Y., Liu, T., Cao, J., Ji, H., Hu, Z., Wu, X., Wang, F., Lu, Y., Chen, N., Zhou, J., Chen, B., Zhou, S., 2024. Effects of seaweed fertilizer application on crop's yield and quality in field conditions in China-A meta-analysis. *PLoS One* 19 (7), e0307517. <https://doi.org/10.1371/journal.pone.0307517>.
- Pulić-Prociak, J., Stoklosa, K., Banach, M., 2015. Nanosilver products and toxicity. *Environ. Chem. Lett.* 13, 59–68. <https://doi.org/10.1007/s10311-014-0490-2>.
- Ribeiro, F., Gallego-Urrea, J.A., Goodhead, R.M., Van Gestel, C.A.M., Moger, J., Soares, A.M.V.M., Loureiro, S., 2015. Uptake and elimination kinetics of silver nanoparticles and silver nitrate by *Raphidocelis subcapitata*: the influence of silver behaviour in solution. *Nanotoxicology* 9, 686–695. <https://doi.org/10.3109/17435390.2014.963724>.
- Sfriso, A.A., Mistri, M., Munari, C., Moro, I., Wahsha, M., Sfriso, A., Juhmani, A.S., 2019. Hazardous effects of silver nanoparticles for primary producers in transitional water systems: the case of the seaweed *Ulva rigida* C. Agardh. *Environ. Int.* 131, 104942. <https://doi.org/10.1016/j.envint.2019.104942>.
- Siddiqui, S., Bielmyer-Fraser, G., 2019. Accumulation and effects of dissolved and nanoparticle silver and copper in two marine seaweed species. *Georg. J. Sci.* 77, 1–17.
- Sinaei, M., Loghmani, M., Bolouki, M., 2018. Application of biomarkers in brown algae (*Cystoseira indica*) to assess heavy metals (Cd, Cu, Zn, Pb, Hg, Ni, Cr) pollution in the northern coasts of the Gulf of Oman. *Ecotoxicol. Environ. Saf.* 164, 675–680. <https://doi.org/10.1016/j.ecoenv.2018.08.074>.
- Tortella, G.R., Rubilar, O., Durán, N., Diez, M.C., Martínez, M., Parada, J., Seabra, A.B., 2020. Silver nanoparticles: toxicity in model organisms as an overview of its hazard for human health and the environment. *J. Hazard Mater.* 390, 121974. <https://doi.org/10.1016/j.jhazmat.2019.121974>.
- Tran, Q.H., Nguyen, V.Q., Le, A., 2013. Silver nanoparticles : synthesis , properties , toxicology, applications and perspectives. *Adv. Nat. Sci. Nanosci. Nanotechnol.* 4, 033001. <https://doi.org/10.1088/2043-6254/aad12b>.
- Turner, A., Brice, D., Brown, M.T., 2012. Interactions of silver nanoparticles with the marine macroalga, *Ulva lactuca*. *Ecotoxicology* 21, 148–154. <https://doi.org/10.1007/s10646-011-0774-2>.
- Valdiglesias, V., 2022. Cytotoxicity and genotoxicity of nanomaterials. *Nanomaterials* 12, 279–290. <https://doi.org/10.3390/nano12040634>.
- Vimbela, G.V., Ngo, S.M., Frazee, C., Yang, L., Stout, D.A., 2017. Antibacterial properties and toxicity from metallic nanomaterials. *Int. J. Nanomedicine* 12, 3941–3965. <https://doi.org/10.2147/IJN.S134526>.
- Wang, H., Ho, K.T., Scheckel, K.G., Wu, F., Cantwell, M.G., Katz, D.R., Horowitz, D.B., Boothman, W.S., Burgess, R.M., 2014. Toxicity, bioaccumulation, and biotransformation of silver nanoparticles in marine organisms. *Environ. Sci. Technol.* 48, 13711–13717. <https://doi.org/10.1021/es502976y>.
- Wei, L., Lu, J., Xu, H., Patel, A., Chen, Z.S., Chen, G., 2015. Silver nanoparticles: synthesis, properties, and therapeutic applications. *Drug Discov. Today* 20, 595–601. <https://doi.org/10.1016/j.drudis.2014.11.014>.
- Xiang, L., Fang, J., Cheng, H., 2018. Toxicity of silver nanoparticles to green algae *M. aeruginosa* and alleviation by organic matter. *Environ. Monit. Assess.* 190, 667. <https://doi.org/10.1007/s10661-018-7022-7>.
- Yin, L., Cheng, Y., Espinasse, B., Colman, B.P., Auffan, M., Wiesner, M., Rose, J., Liu, J., Bernhardt, E.S., 2011. More than the ions: the effects of silver nanoparticles on *Lolium multiflorum*. *Environ. Sci. Technol.* 45, 2360–2367. <https://doi.org/10.1021/es103995x>.
- Zhang, J., Xiang, Q., Shen, L., Ling, J., Zhou, C., Hu, J., Chen, L., 2020. Surface charge-dependent bioaccumulation dynamics of silver nanoparticles in freshwater algae. *Chemosphere* 247, 125936. <https://doi.org/10.1016/j.chemosphere.2020.125936>.